

SLM AND FLAGS FOR BOOSTER OF NSLS-II

O.I. Meshkov, NSU, Novosibirsk, Russia,  
V.V. Smalyuk, V.N. Dorokhov, BINP, Novosibirsk 630090, Russia

## *Abstract*

Set of diagnostics of booster of NSLS-II includes 6 fluorescent screens (flags) and 2 synchrotron light monitors (SLM). The flags will be applied during booster commissioning for closing of the beam turn. They are also useful tool in case of malfunction elimination. SLM will be used as for booster commissioning as for operation. The details of calibration and design of the devices are discussed.

## FLUORESCENT SCREENS

Six fluorescent screens (beam flags) will be used for booster commissioning and troubleshooting. Fluorescent screens with their optics and cameras are used to measure transverse beam profile and position in single-pass mode. A beam image is registered by a CCD camera GC1290.

The thickness of the Cerium-doped Yttrium Aluminum Garnet (YAG:Ce) plate of the screens is 0.1 mm. The plates are produced by Crytur Company (Czech Republic). The beam flag consists of an integrated system of components that can be reconfigured and interchanged, whereby screen can be easily taken out of a UHV-compatible body.

This beam-destructive diagnostics usually plays a key role during commissioning of a machine. The first beam flag is used to adjust the septum and injection kickers to inject a beam into the Booster. To provide correct opera-

tion of the first arc magnets we can observe the beam on the second screen. To close the first turn, the same procedure should be repeated for all the arcs with the beam observation on the next screens. The beam flags are marked in the booster drawings as BR-CSVF1, BR-XSVF1, BR-XSVF2, BR-DSVF1, BR-ISVF1, BR-ISVF2, see Fig. 1.

Expected resolution of the fluorescent screen is about 50  $\mu\text{m}$  within the visible field of 20 mm.

The screen is placed inside a cylindrical volume and move inside and outside of the vacuum chamber. The CCD-camera is placed outside the median plane of the accelerator and is radiation-protected with the lead shield. The screen can move between two fixed positions with pneumatic actuator, inside and outside of the vacuum chamber. The extreme positions are equipped with end switches for control of the flag status. The bottom of the device body will serve as a wake-field shield, when the beam flag is removed out of the chamber. The CCD camera positioning and focusing lens tuning will be performed using the screen mesh, the lead shield will be temporary removed for this operation. Any replacement of the equipment does not need violation of the vacuum

The scattering angle of the electrons after crossing of 0.5 mm of the stainless steel is [1]

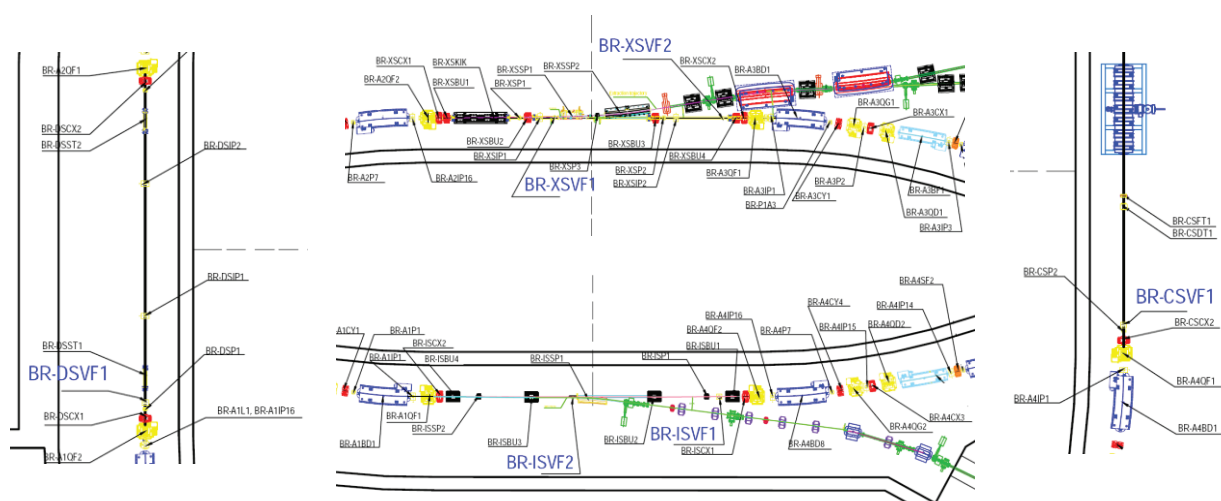


Figure 1: Locations of the beam flags along booster ring.

$$\theta_s = \frac{13.6 MeV}{\beta cp} Z \sqrt{\frac{x}{X_0}} \left[ 1 + 0.0038 \ln\left(\frac{x}{X_0}\right) \right],$$

where  $\beta = v/c$  is the relativistic beta of the electron,  $p$  is its longitudinal momentum,  $MeV/c$ ,  $Z=1$  for electron,  $x = 0.5$  mm is the thickness of the wall and  $X_0 \approx 0.5$  mm is the radiation length for the stainless steel.

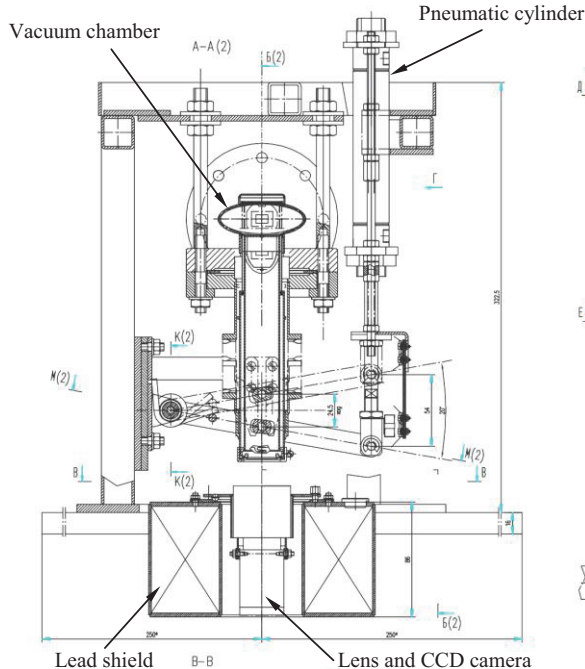


Figure 2: Kinematical scheme of the beam flag.

It corresponds to decrease of the beam footprint on the screen by the value of  $\sigma_s \approx 0.15$  mm at the injection energy  $E_{inj} = 200$  MeV. This enlargement of the beam image is less than the computed beam sizes  $\sigma_x$ ,  $\sigma_y$  and should not distort the output data of the diagnostics. The beam image enlargement is completely negligible at the extraction energy  $E_{ext} = 3$  GeV.



Figure 3: Beam flag at the booster ring

The kinematic scheme and photo of the flag is presented at the Fig. 2, 3.

## FLUORESCENT SCREEN CALIBRATION

We have decided to compare YAG:Ce with other types of phosphors and crystals, which could be applied for the screens (Table 1, Fig. 4)).

Table 1: Crystals, Studied in the Experiments

| Crystal                               | Refr. Index   | Hydroscopic | Mech. prop-  |
|---------------------------------------|---------------|-------------|--------------|
| 1: Al <sub>2</sub> O <sub>3</sub> :Cr | 1.57 (589 nm) | No          | Excellent    |
| 2: BGO                                | 2.15          | No          | Good         |
| 3: CdWO <sub>4</sub>                  | 2.25          | No          | Satisfactory |
| 4: ZnW <sub>04</sub>                  | 2.1-2.2       | No          | Satisfactory |
| 5: YAG:Ce                             | 1.82          | No          | Excellent    |

At this stage of the experiments we were not interested in spatial resolution of the screens. The measurements were done at the electron and positron beam extracted from synchrobetatron B-4M [2]. Beam energy was  $E=354$  MeV, and duration – of about 5 nsec. The beam was extracted from B-4M through separation foil into atmosphere, passed through the examined fluorescent screen and was absorbed in Faraday [3]

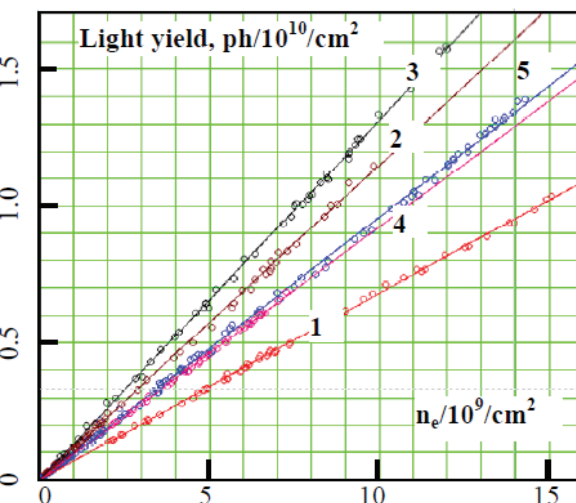


Figure 4: Light yield of the crystals vs beam charge. See Table 1 for key.

At the present time all the flags are installed at the booster ring and remote control of them is provided.

## SYNCHROTRON LIGHT MONITORS (SLM)

The synchrotron radiation (SR) monitor provides routine measurements of transverse beam profiles and beam sizes. It is used for the Booster performance optimization, operation monitoring and various beam physics studies. The monitor has ability to resolve small transverse beam dimension and slow motion with spatial resolution better than 50  $\mu$ m in each plane. The synchrotron radiation monitor consists of a metallic mirror placed inside the vacuum chamber, light output window, image formatting optics and a CCD camera.

Parameters of synchrotron radiation at the extraction energy  $E_{\text{ext}} = 3 \text{ GeV}$  computed for the beam current  $I = 1 \text{ mA}$ , bending radius  $\rho = 8.877 \text{ m}$  and circumference  $C = 158.4 \text{ m}$  are the following:

- ultimate SR angular divergence is  $\theta = 1/\gamma = 1.7 \cdot 10^{-4} \text{ rad}$ ;
- angular divergence of visible SR at  $\lambda = 5000 \text{ \AA}$  is  $\theta_{\text{opt}} \approx 0.62 \left(\frac{\lambda}{\rho}\right)^{1/3} \approx 2.38 \cdot 10^{-3} \text{ rad}$ ;
- cone angle of SR fan in the horizontal plane is  $\theta_r = 10.8 \text{ mrad}$ ;
- critical energy is  $E_c \approx \frac{5.59}{E^3} \rho = 6.75 \text{ keV keV}$ ;
- optical resolution in the vertical direction is  $d_y \approx \frac{\lambda}{2\pi\theta_{\text{opt}}} \approx 0.034 \text{ mm}$ ;
- optical resolution in the horizontal direction is  $d_x \approx \rho \frac{(\theta_{\text{opt}})^2}{2} \approx 0.025 \text{ mm}$ .

The FWHM vertical size of SR spot on the extracting mirror placed at the distance of  $L = 712 \text{ mm}$  is  $d_x \approx 2.36 \cdot \theta \cdot L \approx 0.285 \text{ mm}$  for SR with  $\lambda \approx \lambda_c$ . For the visible part of radiation it has a value of  $d_s \approx 4 \text{ mm}$ . The vertical size of mirror is 24 mm, the maximum allowed deviations at the SR source points are:  $\pm 12 \text{ mm}$  for vertical beam position,  $\pm 16 \text{ mrad}$  for vertical angle, and  $\pm 3.5 \text{ mm}$  for horizontal beam position.

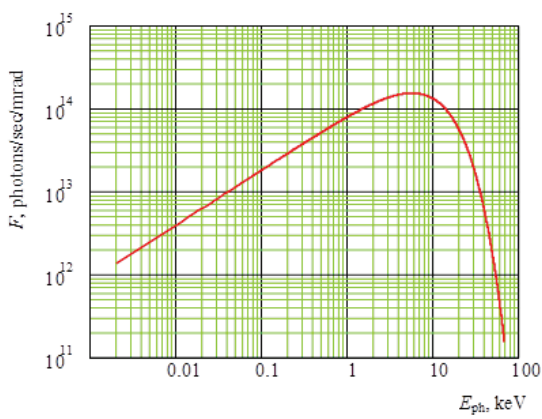


Figure 4: Photon flux of SR from the BD dipole magnet (0.1 % bandwidth).

The spectrum of synchrotron radiation, calculated using [4] for the above-mentioned beam parameters at  $E = 3000 \text{ MeV}$ ,  $I = 1 \text{ mA}$  is presented in Fig. 4. The power of SR on the mirror per one milliradian is  $P_t = 0.42 \text{ W}$ , which corresponds to the total power of  $W_s = 4.54 \text{ W}$ .

The locations of SR extraction out of the vacuum chamber are chosen according to the following considerations:

- maximal vertical beam size;
- maximal free length of the vacuum chamber between the magnets.

As a result, the points of SR generation for output are in the BD dipole magnets (Fig. 5, 6). Two ports of SR output are proposed; the first one is located in the 3<sup>rd</sup> arc, the second one is close to the diagnostic straight section. The second SR output will be used for the Booster commissioning.

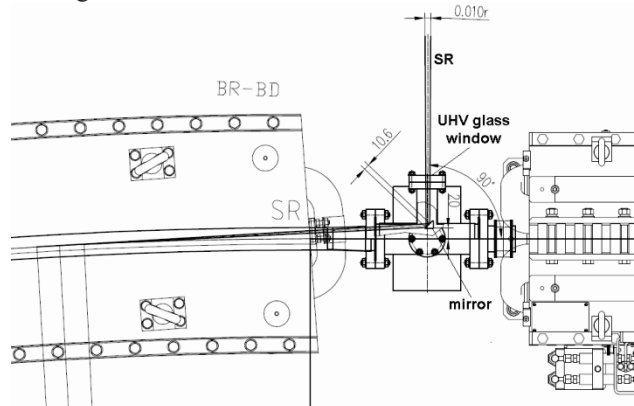


Figure 5: Layout of the SR extraction from BR-A3BD4 magnet.

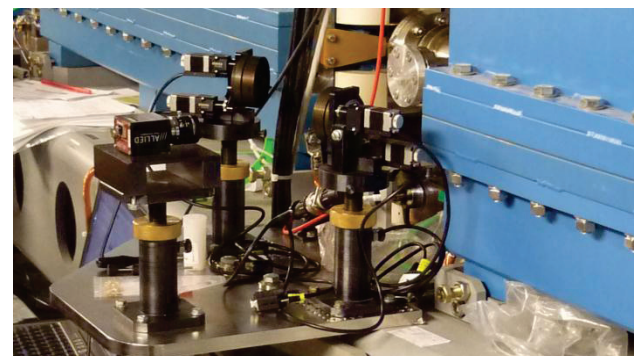


Figure 6: Image formatting optics and CCD camera installed at the booster ring.

## ACKNOWLEDGMENTS

This work is supported in part by the Ministry of Education and Science of the Russian Federation, RFBR (contract № 16.518.11.7003).

## REFERENCES

- [1] H.A. Bête, Molier's Theory of Multiple Scattering, Phys. Rev. 89, 1256(1953)
- [2] V.V. Anashin et al., EPAC98, Stockholm, Sweden, 1998, Vol. 1, p. 400.
- [3] Proceedings of DIPAC09, WEOBE02, Yamburg, 2009.
- [4] <http://physics.nist.gov/MajResFac/SURF/SURF/schwinger.html>